

Review

Processing and Properties of Aluminum and Magnesium Based Composites Containing Amorphous Reinforcement: A Review

Jayalakshmi Subramanian ^{1,2}, Sankaranarayanan Seetharaman ^{1,*} and Manoj Gupta ¹

¹ Department of Mechanical Engineering, National University of Singapore, 9 Engineering Drive 1, Singapore 117576, Singapore;

E-Mails: jayalakshmi.subramanian@gmail.com (J.S.); mpegm@nus.edu.sg (M.G.)

² Department of Mechanical Engineering, Bannari Amman Institute of Technology, Satyamangalam, Tamil Nadu 638401, India

* Author to whom correspondence should be addressed; E-Mail: seetharaman.s@nus.edu.sg; Tel.: +65-6516-2241; Fax: +65-6779-1459.

Academic Editor: Hugo F. Lopez

Received: 27 January 2015 / Accepted: 2 May 2015 / Published: 11 May 2015

Abstract: This review deals with the processing and properties of novel lightweight metal matrix composites. Conventionally, hard and strong ceramic particles are used as reinforcement to fabricate metal matrix composites (MMCs). However, the poor mechanical properties associated with the interfacial de-cohesion and undesirable reactions at (ceramic) particle–(metallic) matrix interface represent major drawbacks. To overcome this limitation, metallic amorphous alloys (bulk metallic glass) have been recently identified as a promising alternative. Given the influential properties of amorphous metallic alloys, their incorporation is expected to positively influence the properties of light metal matrices when compared to conventional ceramic reinforcement. In view of this, a short account of the existing literature based on the processing and properties of Al- and Mg-matrix composites containing amorphous/bulk metallic glass (BMG) reinforcement is presented in this review.

Keywords: aluminum; magnesium; amorphous materials/Bulk Metallic Glass (BMG) reinforcement; processing methods; mechanical properties

1. Introduction

Metallic glasses are novel metallic materials that exhibit superior properties such as high strength (~2 GPa) and elastic strain limit (~2%) [1]. Recently, there have been some attempts to use these metallic glasses as reinforcement in metal matrix composites. Conventionally, metal-matrix composites are made by incorporating hard and strong ceramic reinforcement such as Al₂O₃ or SiC, in the form of fibers, flakes or particles [2]. However, the undesirable reactions and the interfacial de-cohesion at the (ceramic) particle–(metallic) matrix interface often result in poor mechanical properties [3]. In this regard, considering the metastable nature of the amorphous/metallic glass materials, they are considered viable for use as reinforcement in light metal matrices such as Al and Mg with relatively low melting points. Further, the reinforcement/matrix interface being metallic in nature is expected to negate the adverse effects experienced in conventional ceramic reinforced composites [4]. In this respect, the present article will give an in-detail review of the research efforts that have been undertaken so far on the development of amorphous/metallic glass reinforced light-metal matrix composites. In the first section, the preparation and properties of aluminum metal matrix composites containing amorphous reinforcement are presented and the second section deals with that of magnesium matrix composites.

2. Preparation and Characterization of Amorphous/Glass Reinforced Al-Metal Matrix Composites (MMCs)

2.1. Ni-Based Amorphous/Glassy Reinforcements

Lee *et al.* fabricated amorphous/glass reinforced Al-composite for the first time, by reinforcing 20 vol% of Ni-Nb-Ta amorphous alloy (in the form of ribbons) in Al-matrix (Al-356 alloy) using the melt infiltration technique [4]. In this study, the Al-6.5Si-0.25Mg (wt%) alloy was selected as matrix material and the excellent castability of the selected alloy ensured fabrication of defect-free composites by the infiltration process. Here, the Ni-Nb-Ta based Ni_{39.2}Nb_{20.6}Ta_{40.2} (wt%) alloy with excellent thermal stability against crystallization (crystallization onset temperature = 721 °C, which is higher than the liquidus temperature of the A356 alloy = 613 °C) was carefully chosen as the reinforcing material, so as to retain the amorphous structure of the reinforcement. In the first stage, amorphous ribbons (thickness: ~30 μm, width: ~1 mm) of the above mentioned Ni-Nb-Ta alloy were fabricated using the melt spinning process and then cold-pressed (pressure: 16 MPa) into cylindrical preforms (diameter: 9 mm and height: 15 mm) for composite making. In the next stage, the melt infiltration process involved the heating and pressure infiltration of the molten A356 alloy into the prepared amorphous preform. Upon successful synthesis, the structural, thermal, and mechanical properties of the bulk composites were investigated. The results of optical microscopic analysis (Figure 1a) showed the absence of any macro scale defects and showed a homogenous distribution of amorphous reinforcement. Also, no new additional phases were reported in this study which was attributed to the thermal and structural stability of the amorphous reinforcement. Using X-ray diffraction analysis, the crystallographic properties of the composite samples were studied in comparison to that of the amorphous ribbon and the base Al-alloy. The reported X-ray diffractograms are shown in Figure 1b. They show the retention of the amorphous structure of the Ni-Nb-Ta alloy even after the infiltration

process which confirmed the suitability of the infiltration process to fabricate light metal matrix composites containing amorphous particles of high thermal stability. Mechanical property measurements were carried out under indentation and compression loads and the reported properties (Table 1) revealed an increment in strength by amorphous reinforcement addition.

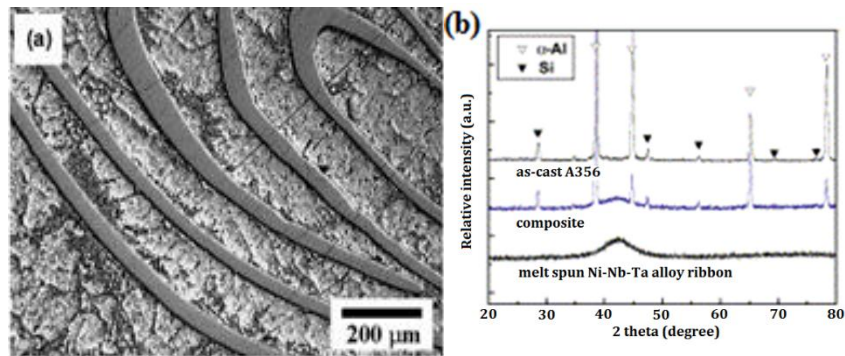


Figure 1. (a) Optical micrographs of Ni-Nb-Ta metallic glass ribbon reinforced A356 alloy based composite; (b) X-ray diffractograms of Ni-Nb-Ta metallic glass ribbon reinforced Al-matrix composite in comparison with the melt spun Ni-Nb-Ta amorphous alloy and as-cast A356 alloy (reprinted from Lee *et al.* 2004 [4], with permission from © Elsevier).

Table 1. Properties of bulk metallic glass (BMG) reinforced Al-MMCs.

Matrix	Reinforcement	Amount	Processing Condition	Hardness (H _v)	Compressive Yield Strength (MPa)	Ultimate Compressive Strength (MPa)	Strain at Fracture (%)	Reference
Al 356	Ni-Nb-Ta	20 vol%	Melt infiltration	-	163	320	16	[4]
Pure Al	Ni ₇₀ Nb ₃₀	30 wt%	Powder Metallurgy (Compaction + Sintering)	-	111	146	-	[5]
Pure Al	Ni ₇₀ Nb ₃₀	30 wt%	Mechanical Alloying + Sintering	-	94	-	-	
Pure Al	Ni ₇₀ Nb ₃₀	30 wt%	Mechanical Alloying + Hot Press	-	106	-	-	[6]
Pure Al	Ni ₆₀ Nb ₄₀	5 vol%	Mechanical Alloying +	74.5	114 (50) *	300 ** (60) *	>50 ** (16.8) *	
Pure Al	Ni ₆₀ Nb ₄₀	15 vol%	Cold Compaction Microwave Sintering +	103.3	125 (75) *	333 ** (85) *	>50 ** (18.0) *	[7]
Pure Al	Ni ₆₀ Nb ₄₀	25 vol%	Hot Extrusion	125.2	155 (102) *	375 ** (120) *	>50 ** (9.5) *	
Pure Al	Zr-Ti-Nb-Cu- Ni-Al	40 vol%	Mechanical Alloying +	-	-	200	-	[8]
Pure Al	Zr-Ti-Nb-Cu- Ni-Al	60 vol%	Hot Extrusion	-	-	250	-	
Al 520	Cu ₅₄ Zr ₃₆ Ti ₁₀	15 vol%	Mechanical Alloying + High Frequency Induction Sintering	-	580	840	14	[9]

Table 1. Cont.

Matrix	Reinforcement	Amount	Processing Condition	Hardness (Hv)	Compressive Yield Strength (MPa)	Ultimate Compressive Strength (MPa)	Strain at Fracture (%)	Reference
Al 6061	Fe-Co based	15 vol%	Powder Metallurgy + High Frequency Induction Sintering	-	167	570	13	[10]
Al 2024	Fe-Nb-Ge-P-C-B	7.2 vol%	Powder Metallurgy + Hot Extrusion	-	403	660	12	[11]
Al 2024	Fe _{49.9} Co _{35.1} Nb _{7.7} B _{4.5} S _{i_{2.8}}	10 vol%	Gas Atomization + Hot Pressing + Hot Extrusion	-	(179) *	(297) *	(7) *	[12]
		20 vol%			(200) *	(320) *	(6.7) *	
		30 vol%			(225) *	(340) *	(5.1) *	
		40 vol%			(229) *	(363) *	(4.7) *	
Al	Mg ₆₅ Cu ₂₀ Zn ₅ Y ₁₀	10 vol%	Ball Milling +	-	203	247	25	[13]
		30 vol%	Hot Pressing		221	323	5.8	

* Number in brackets represents the tensile properties; ** Tests stopped at 50% strain due to equipment limitation.

Following the work of Lee *et al.* [4], Yu *et al.* [5] fabricated Ni₇₀Nb₃₀ metallic glass particle-reinforced Al-metal matrix composite using the powder metallurgy route by sintering below the melting temperature of Al. In this work, the Ni₇₀Nb₃₀ glass particles were prepared by ball milling pure Ni and Nb elemental powders for 20 h. As it is known that most of the metallic glasses have a crystallization temperature lower than the melting point of Al alloys (~933 K), the selection of sintering temperature and time plays an important role in the solid state powder metallurgy processing of bulk metallic glass (BMG) particle reinforced light metal matrix composites. In this study, to avoid the crystallization of amorphous reinforcement, the Al-30 wt% Ni₇₀Nb₃₀ glass particles reinforced composite was compacted at room temperature and sintered at 773 K for 2 h. Microstructural features showed the retention of the amorphous state of the glassy particles after sintering, with no interfacial products. Investigation on the mechanical properties showed an increase in compressive yield and ultimate tensile strengths when compared to pure Al, in addition to a 69% increase in the Young's modulus value. Eckert *et al.* [6] also used Ni₆₀Nb₄₀ (at%) amorphous powder reinforcement. The amorphous Ni₆₀Nb₄₀ powder (30 wt%) prepared by mechanical alloying was reinforced in pure Al by mixing, sintering, hot pressing, and hot extrusion. Sintering was performed at ~823 K which is below the recrystallization temperature of Ni₆₀Nb₄₀ amorphous powder. Results of X-ray diffraction analysis conducted on the composite specimen confirmed the retention of the amorphous structure of Ni₆₀Nb₄₀ (at%) reinforcement and only the crystalline peaks of Al were present. The results of indentation and compression tests (Table 1) revealed superior mechanical properties (in all conditions), which was attributed to the inherent superior strength of the Ni₆₀Nb₄₀ (at%) amorphous alloy (strength ~2GPa and hardness ~800 Hv).

Recently, Jayalakshmi *et al.* [7] prepared Al-matrix composites containing different amounts of Ni₆₀Nb₄₀ (at%) amorphous reinforcement using rapid microwave sintering assisted powder metallurgy technique. The amorphous Ni₆₀Nb₄₀ alloy reinforcement required for the study was initially prepared

by ball milling the elemental Ni and Nb metal powder in a planetary ball milling machine for 87 h. The ball milling parameters include milling speed of 200 rpm, and ball to powder ratio of 3:1. In the next stage, the required amount (5, 15, 25 vol%) of the prepared amorphous reinforcement was blended with pure Al powder in a planetary ball milling machine (without balls) for 1 h at 200 rpm. The blended composite powder mixture was then cold compacted into a cylindrical billet of diameter 36 mm and height 50 mm. The compacted billets were then sintered using the microwave sintering approach which employed the combined action of microwave and a microwave couple external heating source to rapidly heat the composite materials (to 823 K, which is less than the crystallization temperature of Ni₆₀Nb₄₀ amorphous alloy) in a short period of time (12 min). The sintered billets were then soaked at 673 K for 1 h and hot extruded at 623 K into cylindrical rods of diameter 8 mm on which the structural and mechanical property characterization were performed. The results of structural characterization (SEM microscopy and X-ray analyses) revealed the retention of the amorphous structure and the uniform distribution of the reinforcement without any interfacial reaction products (Figure 2). Structural dilatation and change in the aspect ratio of reinforcement in 25 vol% amorphous particle reinforced composite was also observed. The observed features were attributed to the local stress variations and the temperature gradients within the composite arising *in-situ* during hot extrusion, due to reduced inter-particle spacing.

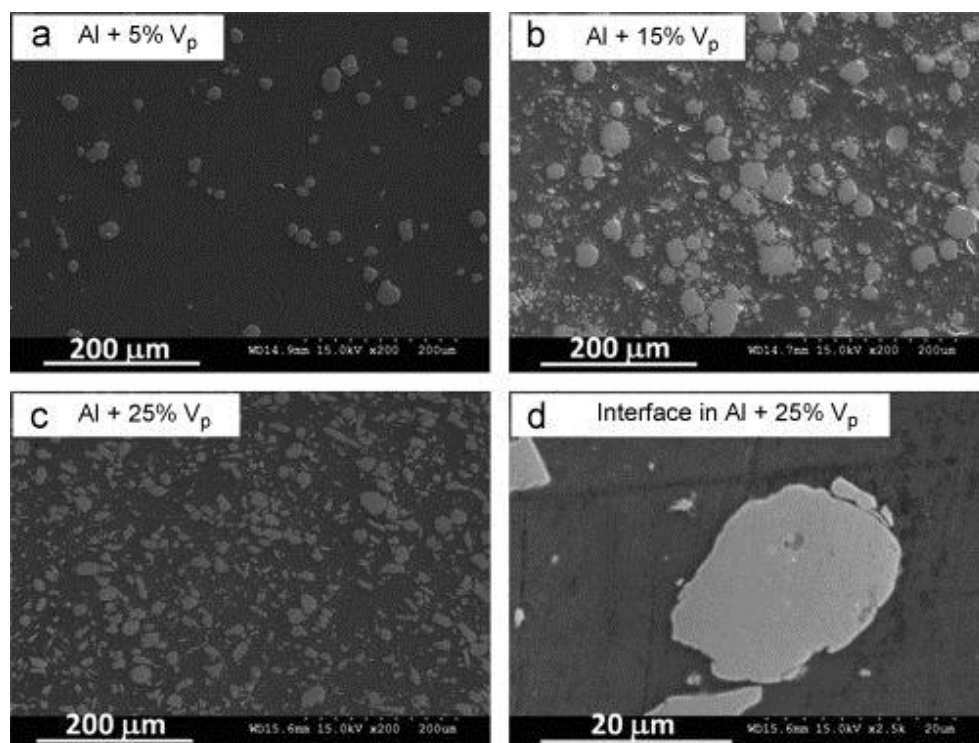


Figure 2. Cont.

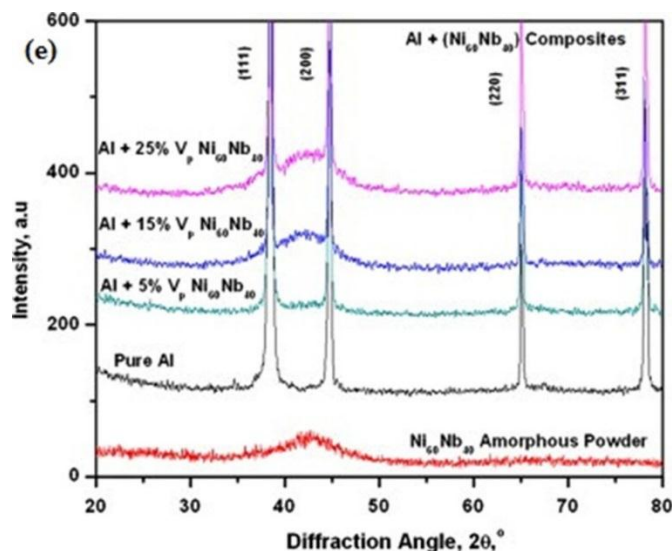


Figure 2. Results of microstructural (a–d) analyses conducted on Al-matrix composites reinforced with $\text{Ni}_{60}\text{Nb}_{40}$ metallic glass powder, Results of X-ray diffraction analyses (e) conducted on Al-matrix composites reinforced with $\text{Ni}_{60}\text{Nb}_{40}$ metallic glass powder (reprinted from Jayalakshmi *et al.* 2014 [7], with permission from © Elsevier).

Electrical resistivity measurements were also conducted on pure Al and its composite samples. The results showed higher resistivity values for composites due to the disordered structure of the amorphous phase. However, these values were found to be less than that of the amorphous Ni-Nb alloys. The reported mechanical properties under indentation, tension, and compression loads are listed in Table 1. When compared to pure Al, the micro-hardness value of 25 vol% composite was increased by ~130%. Compression test results showed ~45%–100% enhancement in compression yield strength without fracture. The reported flow curves are shown in Figure 3. Further, it is also worth mentioning that the long extrusions obtained in this study were sufficient to investigate the tensile properties (gauge length 25 mm, diameter: 5 mm) and the report on the tensile behavior of amorphous alloy/glass-reinforced composites was the first of its kind. It showed that the increment in strengths (both yield strength and ultimate strength) did not follow an increasing trend with reinforcement volume fraction. It showed that a minimum critical volume fraction of reinforcement was required for strength enhancement. A maximum increase in strength by ~60% was obtained in 25 vol% composite. Unlike compression test, the tensile test results showed ductility reduction (however not drastic as ceramic particle reinforced Al-MMCs) due to amorphous particle reinforcement addition.

The microscopic analysis of tension test failed samples (Figure 4) showed prominent ductile features and good interfacial bonding between the matrix and reinforcement. Particle breakage was also reported in 25 vol% composite.

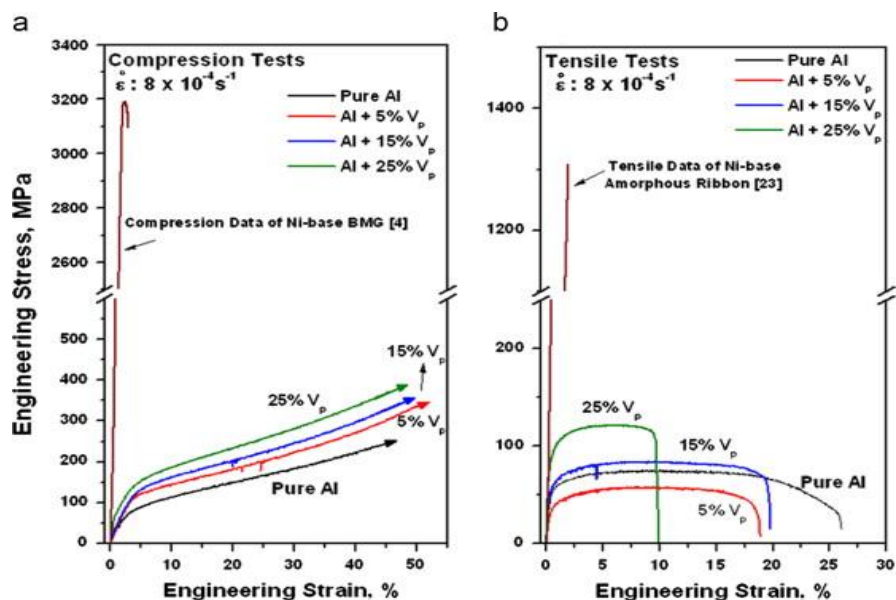


Figure 3. Stress-strain curves of Al-Ni₆₀Nb₄₀ composites under (a) compression and (b) tension loads (reprinted from Jayalakshmi *et al.* 2014 [7], with permission from © Elsevier).

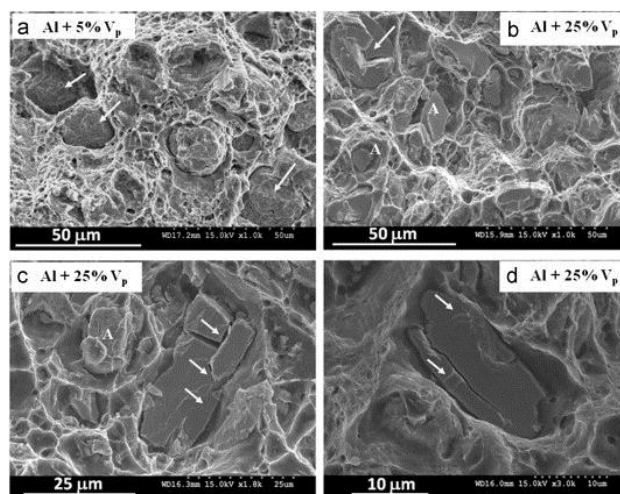


Figure 4. (a,b) Low magnification and (c,d) high magnification fractographs of Al-Ni₆₀Nb₄₀ composites fractured under tensile loads. White arrows indicate better interfacial bonding between particle and matrix with no particle debonding in (a & b), small sized particles remaining intact marked as ‘A’ in (b & c), high aspect ratio particles undergoing multiple cracking and fracture in (c) and vein patterns caused by strain localization in amorphous particles in (d) (reprinted from Jayalakshmi *et al.* 2014 [7], with permission from © Elsevier).

2.2. Zr-Based Amorphous/Glassy Reinforcements

Scudino *et al.* [8] reported the synthesis, structure and compressive behavior of Zr-based metallic glass particle reinforced Al-matrix composites. The Zr₅₇Ti₈Nb_{2.5}Cu_{13.9}Ni_{11.1}Al_{7.5} (at%) BMG reinforcement required for the study was prepared by ball-milling the elemental Zr, Ti, Nb, Cu, Ni, and

Al powder for 120 h under argon atmosphere, with a ball to powder ratio of 13:1 and milling speed of 150 rpm. For making the composites, 40 and 60 vol% of the prepared amorphous powder was mixed with pure Al powder and the powder mixture was consolidated by hot pressing followed by hot extrusion. An extrusion ratio of 6:1 was employed and the extrusion was performed under argon atmosphere at a temperature 673 K, which is slightly lower than the crystallization temperature range (716–757 K) of the metallic glass reinforcement. The structural properties of the developed Al/Zr-BMG composites were investigated using X-ray diffraction and electron microscopy. The results of X-ray diffraction studies indicated the presence of only pure Al-crystalline peaks and the retention of the reinforcements' amorphous structure which confirmed that the crystallization of amorphous reinforcement was completely avoided during the hot pressing and extrusion. The SEM micrographs (Figure 5) showed no porosity and uniform distribution of the reinforcement particles. Particle clustering was also seen in the high volume fraction of amorphous reinforcement addition.

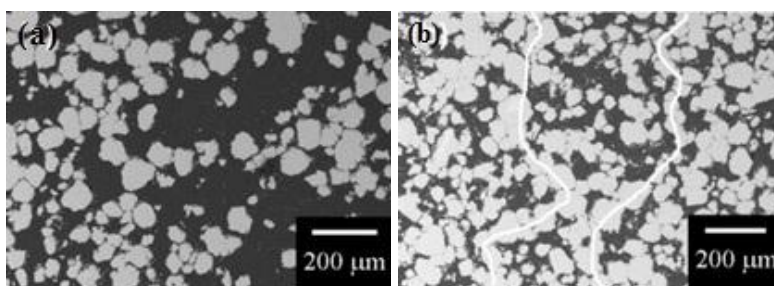


Figure 5. Scanning electron microscopy (SEM) micrographs of (a) 40 vol% and (b) 60 vol% Zr-based glassy particles reinforced Al-matrix composites. White lines in (b) represent the continuous network of particles, (reprinted from Scudino *et al.* 2009 [8], with permission from © Elsevier).

The results of compressive properties reported in comparison to that of the melt spun $Zr_{57}Ti_8Nb_{2.5}Cu_{13.9}Ni_{11.1}Al_{7.5}$ ribbon and pure Al showed that the composite reinforced with 60% reinforcement exhibited superior strength (however less than the amorphous Zr-based ribbon) and work softening behavior. The microscopic features of the fractured samples investigated using scanning electron microscopy (SEM) (Figure 6) showed cracks in the reinforcing particles which occurred parallel to the compression direction. However, the Al matrix underwent large plastic deformation and displayed dimple rupture, which are both indicative of ductile fracture.

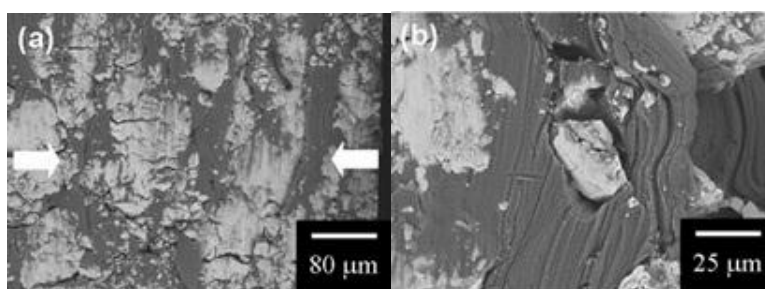


Figure 6. Fractographs of Zr-based metallic glass reinforced Al composites. (a) Low magnification image with loading direction indicated by arrow; (b) particle breakage (reprinted from Scudino *et al.* 2009 [8], with permission from © Elsevier).

2.3. Cu-Based Amorphous/Glassy Reinforcements

Cu-based glassy material reinforced in Al-A520 alloy were developed by Dudina *et al.* [9] using high frequency induction sintering. In this study, the $\text{Cu}_{54}\text{Zr}_{36}\text{Ti}_{10}$ (at%) metallic glass ribbons were prepared by the arc melting/melt spinning process. The prepared amorphous alloy ribbons were then cut and ball-milled for 24 h. The cut ribbons were then mixed together with the Al-matrix alloy in a vibratory mill for 8 h. The composite powder mixture was processed using high frequency induction sintering at a temperature just below the crystallization temperature of the amorphous alloy. The processed composite materials were subjected to X-ray, electron microscopy and compression analysis. While the results of X-ray diffraction analysis indicated no additional phases and transformation of the amorphous phase, electron microscopic observations revealed uniform distribution of the amorphous phase with no preferred orientation. The compressive stress-strain curves as shown in Figure 7 (properties listed in Table 1) revealed promising strength enhancement by efficient load transfer and grain refinement. This was accompanied by a slight reduction in fracture strain. The fracture morphology of the compression test failed specimen indicated no metallic glass particle de-bonding from the matrix (Figure 7b,c).

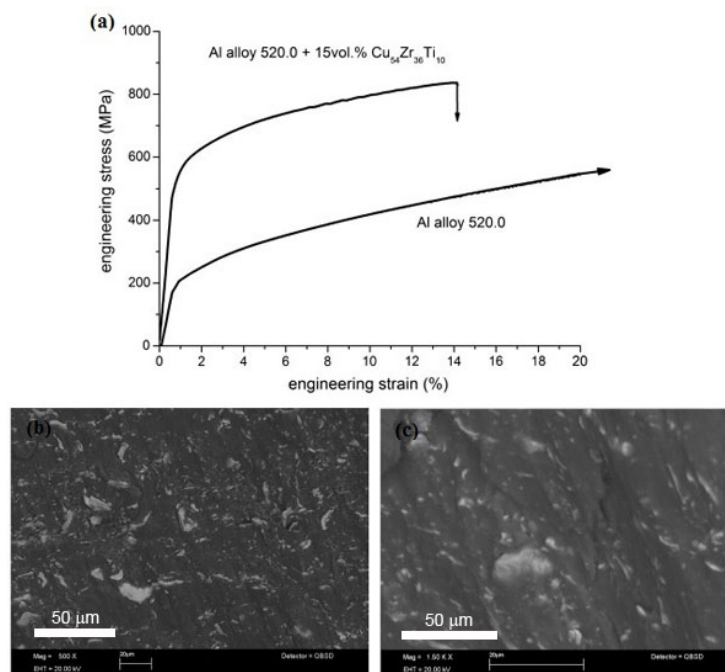


Figure 7. (a) Compression stress-strain curves and (b,c) fractographic evidences of 15 vol% $\text{Cu}_{54}\text{Zr}_{36}\text{Ti}_{10}$ glassy particle reinforced A520 alloy composite (reprinted from Dudina *et al.* 2010 [9], with permission from © Elsevier).

2.4. Fe-Based Amorphous/Glassy Reinforcements

Fujii *et al.* [10] fabricated Fe-based ($\text{Fe}_{72}\text{B}_{14.4}\text{Si}_{9.6}\text{Nb}_4$) metallic glass particle reinforced Al-based composite materials using the friction stir processing method. The selection of the Fe-based metallic glass particle as reinforcement in this study was based on the fact that the glass transition temperature is relatively higher than the welding temperature (673–723 K) of the Al alloys. For the base matrix

material, pure Al plates (1050-H24) with dimension $300 \times 70 \times 5 \text{ mm}^3$ were used. Structural and mechanical property measurements were performed and the results revealed coarsening of Al-grains due to the dispersion of Fe-based BMG particles. Further, it was also reported that dispersion of Fe-BMG particles had little effect on the hardness, although the results of hardness measurements showed improvement. This was attributed to the formation of $\text{Al}_{13}\text{Fe}_4$ precipitates in the stir zone due to the reaction between pure Al and Fe based metallic glass.

Aljerf *et al.* [14] prepared $[(\text{Fe}_{0.5}\text{Co}_{0.5})_{75}\text{B}_{20}\text{Si}_5]_{96}\text{Nb}_4$ amorphous alloy reinforced Al6061 alloy composites using the high frequency induction sintering assisted powder metallurgy method. In this study, Fe-Co based amorphous alloy ribbons of the above mentioned composition were first ball-milled with Al-alloy and the Al/Fe-BMG composite mixture was then densified using induction sintering at 828 K. Similar to earlier studies, DSC and X-ray diffraction analyses were used to comprehend the crystallographic nature of the amorphous reinforcement and the results confirmed the retention of the amorphous structure in the composites (Figure 8). The flow curves under compression (Figure 9) clearly highlight the enhancement in strength properties due to amorphous reinforcement addition. The reported mechanical properties are listed in Table 1.

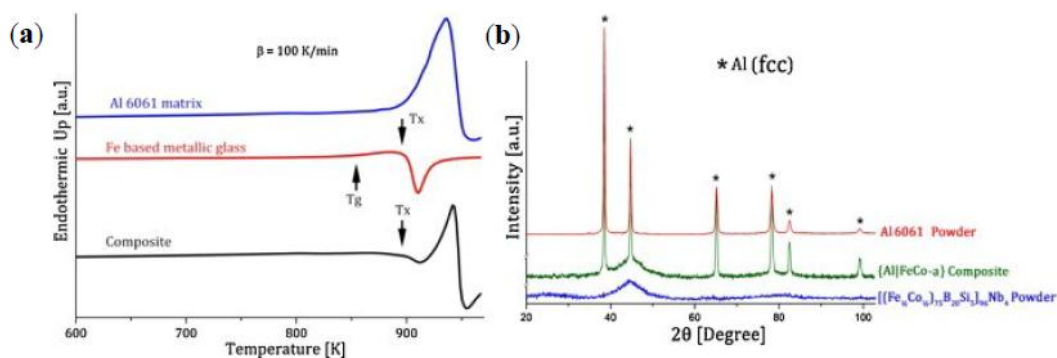


Figure 8. (a) DSC thermograms and (b) X ray diffractograms of Al matrix composite reinforced with Fe-based metallic glass compared to Al 6061 alloy and the Fe-based metallic glass powder (reprinted from Aljerf *et al.* 2012 [14], with permission from © Elsevier).

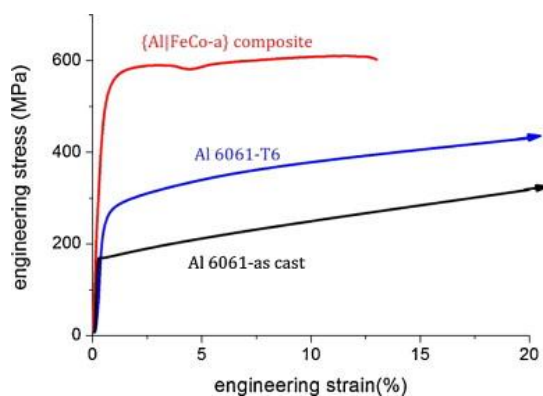


Figure 9. Compression flow curves of Al matrix composite reinforced with Fe-based metallic glass compared to as cast and heat treated Al 6061 alloy (reprinted from Aljerf *et al.* 2012 [14], with permission from © Elsevier).

Zheng *et al.* [11] produced Fe-based BMG particle reinforced 2024 Al-alloy composite using the powder metallurgy method. The Al 2024 alloy matrix and the amorphous $\text{Fe}_{73}\text{Nb}_5\text{Ge}_2\text{P}_{10}\text{C}_6\text{B}_4$ reinforcement materials required, were initially prepared using gas and water atomization respectively. The prepared powders were then ball milled under an argon atmosphere to fabricate the composite powder. Milling parameters include ball to powder ratio of 10:1, sun-disk rotation speed of 280 rpm, planetary-disk rotation speed of 480 rpm, process control agent of stearic acid and argon protective atmosphere. The composite powder mixture was then consolidated and sintered at 823 K, 400 MPa in a 20 mm diameter stainless steel die using induction heating for 30 min. The sintered billet was hot extruded at 823 K at an extrusion ratio of 10:1. Structural characterization showed the distribution of refined amorphous particles and the nanostructure Al-2024 matrix with clear interface between the matrix and amorphous reinforcement (Figure 10). Compression property measurements conducted on the composite samples showed enhanced yield and fracture strength resulting from the nanostructure of the Al-matrix and the uniform distribution of the amorphous reinforcement particles. In a recent study, Marko *et al.* [12] reinforced Al-2024 alloy with different volume fractions of gas atomized $\text{Fe}_{49.9}\text{Co}_{35.1}\text{Nb}_{7.7}\text{B}_{4.5}\text{Si}_{2.8}$ glassy particles using the powder metallurgy method by hot pressing (for 10 min at 673 K, 500 MPa) followed by hot extrusion at the same temperature. Given that the crystallization temperature of the glass reinforcement is ~ 873 K, the sintering temperature was far below the crystallization temperature and avoided crystallization of the glassy particles during sintering. This is yet another work that after ref. [7] investigated the room temperature tensile properties which indicated a 27% and 20% increase in yield and ultimate strengths respectively (listed in Table 1), when compared to the unreinforced alloy matrix. The ductility of the glass particle reinforced composite (range between 5% and 10%) was lower than that of the unreinforced alloy. Nevertheless, the glass particle reinforced composites have a definite advantage over the conventional ceramic reinforced composites, as the conventional composites usually have negligible/no ductility.

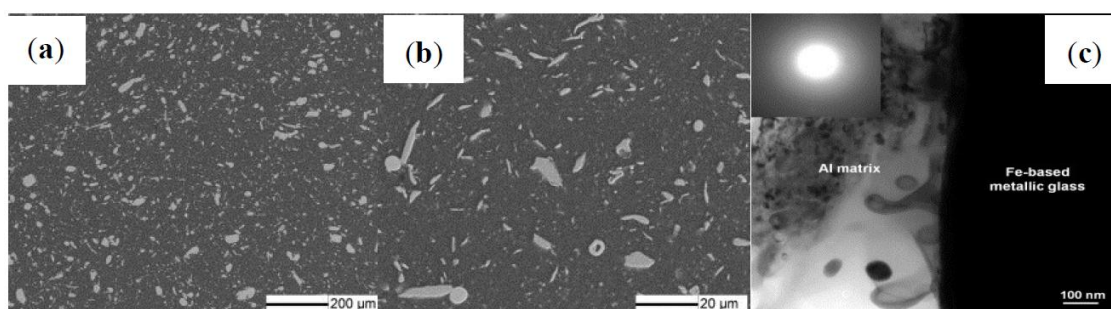


Figure 10. SEM micrographs of Al 2024 alloy reinforced with Fe based metallic glass. (a) Low magnification and (b) high magnification; (c) TEM image showing the interfacial characteristics (reprinted from Zheng *et al.* 2014 [11], with permission from © Elsevier).

2.5. Mg-Based Amorphous/Glassy Reinforcements

Wang *et al.* [13] reinforced $\text{Mg}_{65}\text{Cu}_{20}\text{Zn}_5\text{Y}_{10}$ (at%) glassy particles in pure Al matrix. Injection cast $\text{Mg}_{65}\text{Cu}_{20}\text{Zn}_5\text{Y}_{10}$ metallic glass rods were ball-milled to produce metallic glass powder particles. 10 and 30 vol% of the particles were mixed with pure Al powder and ball-milled to form composite powder (for 10 h with a ball-to-powder ration of 10:1). Uniaxial hot pressing was used to compact the

composite powder in a vacuum at 453 K (falls in the super-cooled liquid region of the Mg-glassy particles) and 700 MPa. Uniform distribution of the glassy particles and good interfacial characteristics were observed. The room temperature compressive properties showed a yield strength increment by a factor of ~ 3 (203 MPa) in the 10 vol% composite (when compared to the unreinforced Al), along with a compressive deformation of $\sim 25\%$ (Table 1). Theoretical strength estimation using modified shear lag (MSL) model was used to explain the strengthening effect which showed good agreement with the experimental data. It was concluded that dislocation strengthening was the dominant strengthening mechanism in the developed composites.

3. Preparation and Characterization of Amorphous/Glass Reinforced Mg-MMCs

Dudina *et al.* [15] initiated the work on reinforcing amorphous/metallic glass in magnesium matrix. The effect of 15 vol% Vitraloy 6, *i.e.*, $Zr_{57}Nb_5Cu_{15.4}Ni_{12.6}Al_{10}$ amorphous alloy reinforcement in AZ31 Mg-alloy was investigated. The composite materials were prepared by using high frequency induction sintering under pressure. In the first stage, Zr-based metallic glass ribbons (prepared by induction melting followed by melt spinning) were cut into pieces and ball-milled in a low speed vibratory mill to prepare amorphous powder particles. The milling was performed for 15 h under an argon atmosphere. In the next stage, the ball milled Zr-based BMG powder (15 vol%) was mixed and milled with the cut ribbons of Mg-alloy. The milled composite powder mixture was then consolidated by using high frequency induction sintering under pressure (50 MPa) at a temperature of 713 K for 120 s. Similar to Al/BMG metal matrix composites, the selection of the sintering temperature was based on the crystallization temperature of Vitraloy 6 metallic glass reinforcement. The consolidated bulk Mg/Zr-BMG composite materials were then characterized for their structural and mechanical properties. Structural investigations involved X-ray diffraction and electron microscopy analyses. The results (Figure 11) revealed the retention of the reinforcement's amorphous structure and the uniform dispersion of the amorphous reinforcement without any interfacial reaction products or pores. This confirms the sound consolidation of the powder materials.

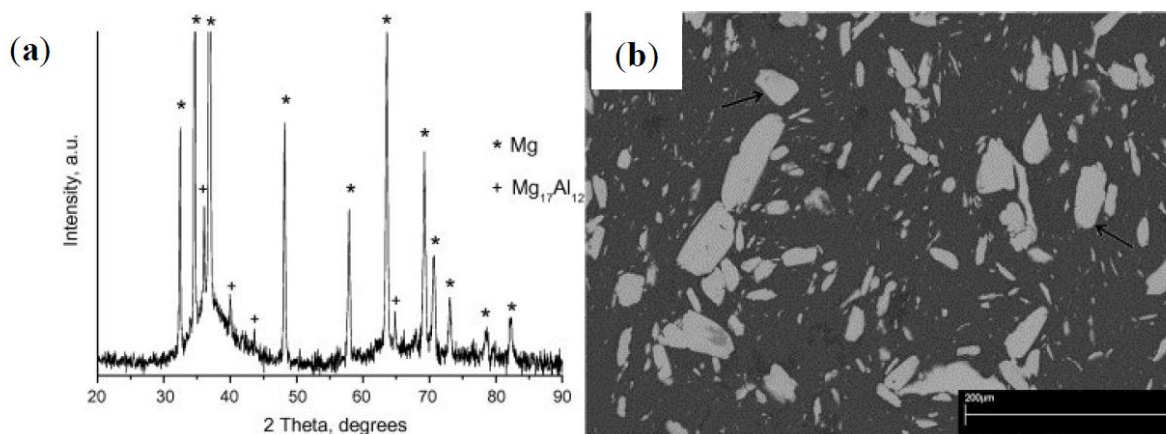


Figure 11. (a) X-ray diffractograms and (b) SEM micrograph of Zr-based glassy particle reinforced AZ91 Mg-alloy composite prepared by high frequency induction heating under pressure. Metallic glass particles are marked with black arrows in (b) (reprinted from Dudina *et al.* 2009 [15], with permission from © Elsevier).

Mechanical property measurements under indentation and compression loads were performed on samples 4 mm long and $2 \times 2 \text{ mm}^2$ cross section. The reported results (Table 2) indicated a significant enhancement in strength properties due to the efficient load transfer and dislocation strengthening.

Table 2. Properties of BMG reinforced Mg-MMCs.

Matrix	Reinforcement	Amount	Processing Condition	Hardness (H_v)	Compressive Yield Strength (MPa)	Ultimate Compressive Strength (MPa)	Strain at Fracture (%)	Reference
AZ 91	Zr-Nb-Cu-Ni-Al	15 vol%	Ball Milling + High Frequency Induction Sintering	123	325	542	10.5	[15]
Pure Mg	Ni-Nb	3 vol%	Ball Milling + Microwave Sintering + Hot Extrusion	62	85	283	17.6	[16]
		5 vol%		84	135	320	18.4	
		10 vol%		95	90	322	17.2	
Pure Mg	Ni-Ti	3 vol%	Ball Milling + Microwave Sintering + Hot Extrusion	49	67 (94) *	291 (144) *	15.9 (8.8) *	[17]
		5 vol%		62	89 (127) *	368 (183) *	15.1 (6.5) *	
		10 vol%		66	102 (148) *	417 (178) *	14.9 (2.0) *	

* Number in brackets represents the tensile properties.

Pure Mg-based composite materials reinforced with varying volume fractions of $\text{Ni}_{60}\text{Nb}_{40}$ (at%) metallic glass particles were synthesized by Jayalakshmi *et al.* [16] using the blend-press-sinter based powder metallurgy method. In the first stage, the amorphous $\text{Ni}_{60}\text{Nb}_{40}$ reinforcement required for the study was prepared by ball-milling. The processing details were similar to that mentioned in Jayalakshmi *et al.* [7]. In the next stage, the required amount (3, 5, 10 vol%) of $\text{Ni}_{60}\text{Nb}_{40}$ BMG reinforcement was mixed with pure Mg powder and the mixture was blended in a planetary ball mill for 1 h. This was followed by the densification of the blended composite powder using uniaxial cold compaction and rapid microwave sintering. A sintering time of 12 min 30 s was selected for microwave sintering so as to reach the sintering temperature of 823 K, which is below the crystallization temperature of the $\text{Ni}_{60}\text{Nb}_{40}$ reinforcement. The sintered billets were then hot extruded at 623 K into cylindrical rods of 8 mm diameter on which the structural and mechanical property investigations were performed. The results of structural characterization by X-ray analysis, optical and electron microscopy revealed matrix grain refinement (Figure 12), uniform distribution of reinforcement at low volume fraction and agglomeration at high volume fractions (Figure 13), absence of interfacial reaction production (Figure 13d) and the retention of the reinforcement's amorphous structure at all volume fractions (Figure 14a). The results of X-ray analyses also indicated the influence of the amorphous reinforcement in changing the dominant crystallographic orientation of the Mg-matrix (Figure 14b). It was reported that the basal planes of the composites were not aligned entirely parallel to the extrusion as generally would be in the case of extruded magnesium materials.

The results of micro-hardness and compression tests (listed in Table 2) showed a remarkable increment with increasing amount of amorphous reinforcement. This behavior was attributed to the inherent high hardness, strength and elastic strain limit of the amorphous reinforcement.

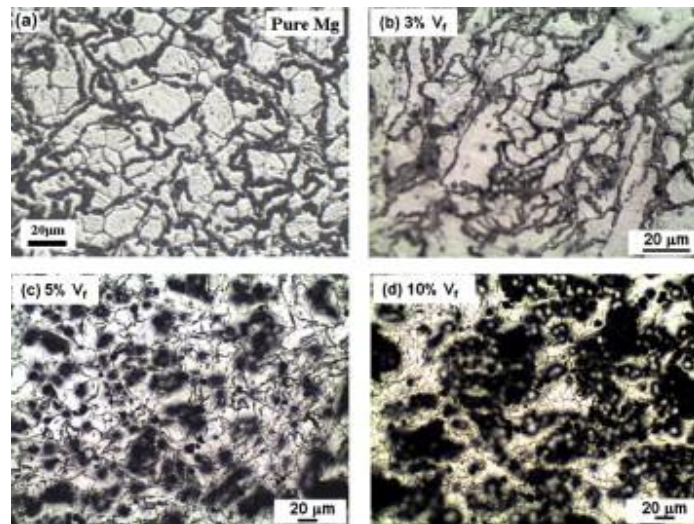


Figure 12. (a) Grain characteristics of pure Mg, and (b–d) its composite reinforced with different amounts of Ni₆₀Nb₄₀ amorphous reinforcement (reprinted from Jayalakshmi *et al.* 2014 [16], with permission from © Elsevier).

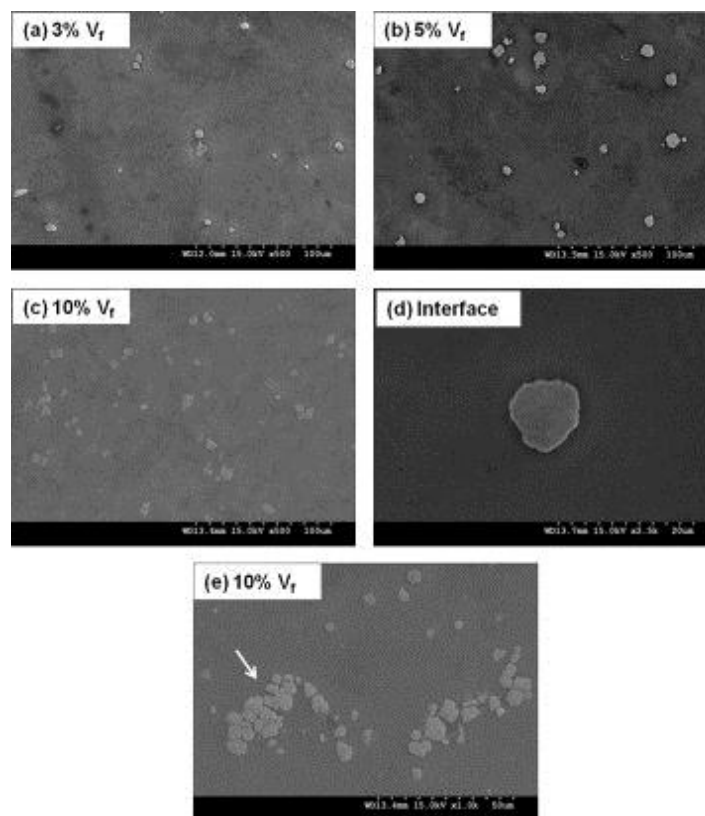


Figure 13. SEM images showing the distribution of Ni₆₀Nb₄₀ amorphous particles in Mg matrix composites. White arrow in (e) represents clustering of particles. (reprinted from Jayalakshmi *et al.* 2014 [16], with permission from © Elsevier).

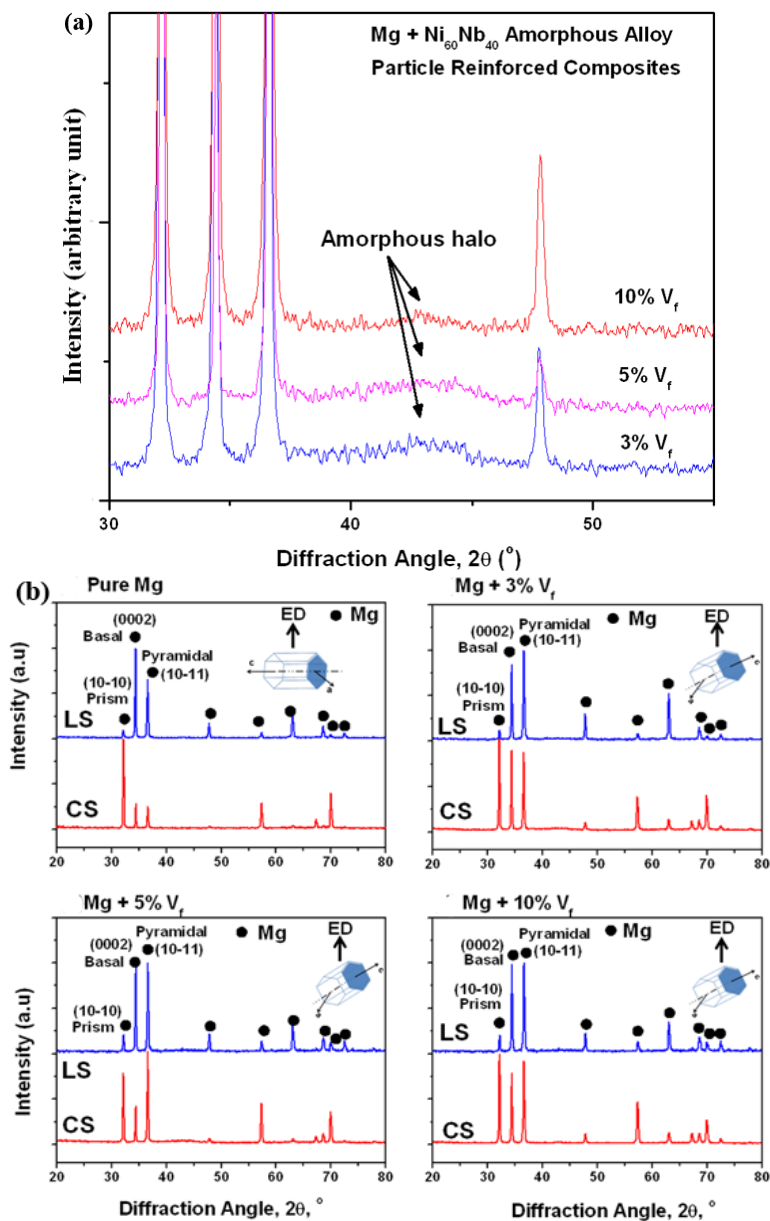


Figure 14. (a) XRD diffractograms of Mg-Ni₆₀Nb₄₀ composites showing the retention of amorphous structure at all volume fractions and (b) change in crystal orientation due to amorphous reinforcement addition. (reprinted from Jayalakshmi *et al.* 2014 [16], with permission from © Elsevier).

Recently, pure Mg reinforced with varying volume fractions of Ni₅₀Ti₅₀ (at%) were fabricated using the microwave sintering assisted powder metallurgy technique [17]. The Ni₅₀Ti₅₀ amorphous reinforcement used in this study was prepared by ball milling the Ni and Ti powder particles for 55 h in a planetary ball milling machine. The ball milling parameters were similar to those used in reference [16]. For composite fabrication, the required amounts (3, 6 and 10 vol%) of the prepared Ni₅₀Ti₅₀ amorphous reinforcement were mixed with pure Mg powder and the composite mixture was then cold compacted in an isostatic press. The compacted billet was then densified using microwave sintering. The sintered composite materials were then hot extruded into cylindrical rods and the samples cut from the cylindrical rods were subjected to X-ray, electron microscopy and mechanical property

characterization. The SEM observations indicated a fair distribution of amorphous reinforcements with a clear matrix/reinforcement interface (Figure 15).

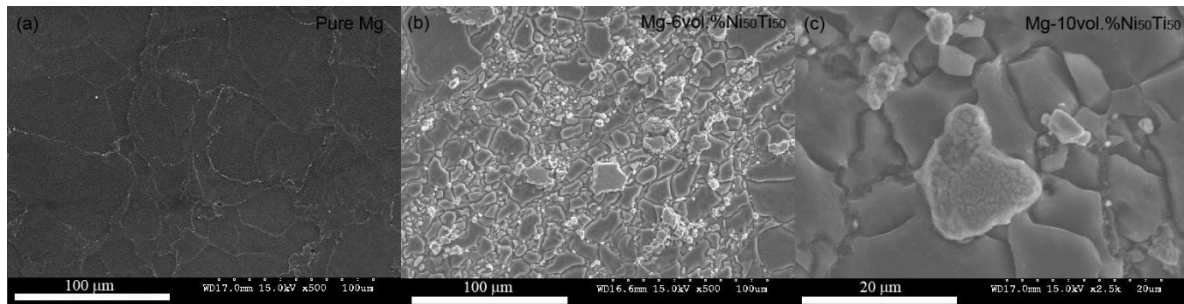


Figure 15. SEM micrographs showing the microstructural characteristics of: (a) pure Mg and its composite containing different amounts of Ni₅₀Ti₅₀ amorphous reinforcement (b,c). (reprinted from Sankaranarayanan *et al.* 2015 [17], with permission from © Elsevier).

The reported mechanical properties are listed in Table 2 which indicated superior strength properties due to amorphous Ni₅₀Ti₅₀ reinforcement addition (Figure 16). The tensile properties of such amorphous particle reinforced magnesium composites were reported for the first time in the case of Ni₅₀Ti₅₀ amorphous particles reinforced magnesium composites. The results showed ~98% increase in tensile yield strength and ~50% increase in the ultimate strength. While the tensile ductility was adversely affected, the reported properties were comparable or superior to that of ceramic particle reinforced Mg-MMCs.

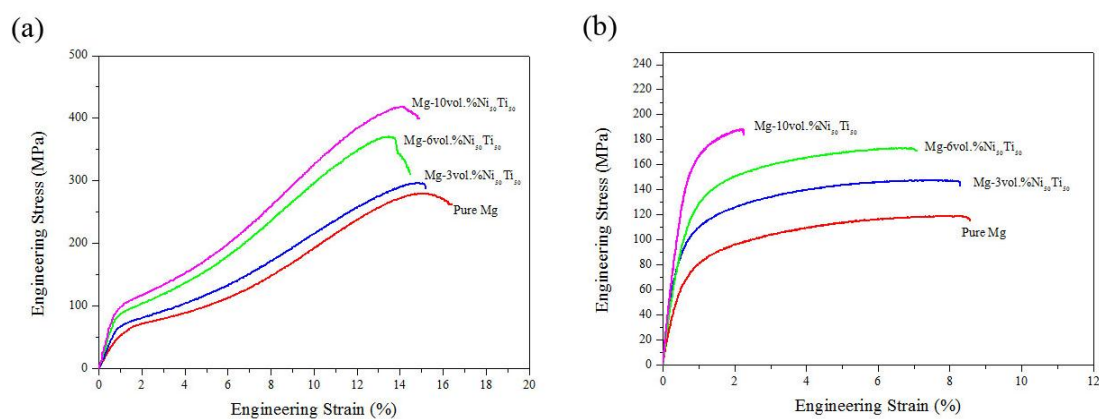


Figure 16. Engineering stress-strain curves of the developed Mg-composites under (a) compressive loading (b) tensile loading (reprinted from Sankaranarayanan *et al.* 2015 [17], with permission from © Elsevier).

The microscopic features of tension test failed samples of Ni₅₀Ti₅₀ particle reinforced Mg-composites were studied in comparison to pure Mg as shown in Figure 17. It revealed dominant quasi-cleavage fracture in both pure Mg and its composites. Sparse particle segregation (debonding) features were also reported in Mg/Ni₅₀Ti₅₀ composites.

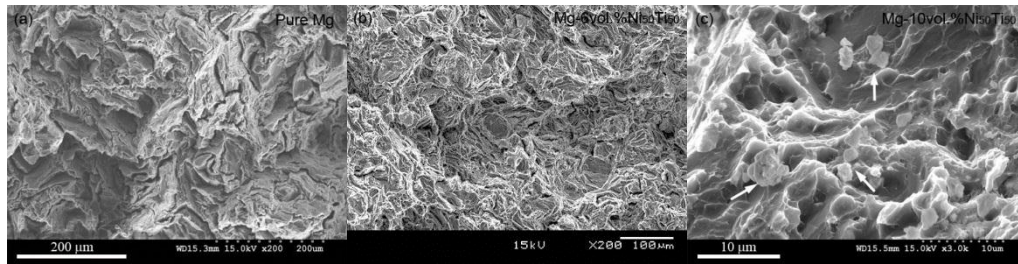


Figure 17. Representative tensile fractographs showing typical cleavage mode fracture in: (a) pure Mg and (b) Mg-6 vol% Ni₅₀Ti₅₀ and (c) prominent particle segregation in Mg-10 vol% Ni₅₀Ti₅₀. White arrows represent fine amorphous particles. (reprinted from Sanakranarayanan *et al.* 2015 [17], with permission from © Elsevier).

4. Influence of Processing Method on the Mechanical Properties

Figure 18 compares the compressive properties of some of the amorphous alloy/metallic glass reinforced composites produced by different methods (as explained in the preceding paragraphs). Considering that in the graph (y-axis) the strength is normalized, the mechanical properties of the composites seem to be dominated by the processing method. Those composites produced by high frequency induction sintering exhibit the highest strength properties, irrespective of the matrix or reinforcement volume fraction. The high frequency induction sintering method is a rapid sintering method with high-temperature exposure and application of pressure over a short duration of time. Amongst the strength of the three composites produced by the high frequency induction sintering method, composites with Mg- and Fe-based glassy particles exhibit the highest strength, which could be due to the higher thermal stability, and enhanced glass formation characteristics of the alloy that may impart a better structural stability during processing, which would in turn improve the mechanical properties. The next best properties are observed in those composites produced by another unconventional rapid sintering method, *i.e.*, microwave sintering, followed by hot extrusion. The method can also produce composites in larger dimensions such that the tensile behavior of the composites can also be studied. Composites produced by this method also show enhanced mechanical properties. These results highlight the fact that rapid sintering is essential to achieve an improved strengthening effect for composites reinforced with amorphous alloy/metallic glass reinforcements, as they can minimize interaction time with the matrix, promote rapid sintering, reduce porosity/defects, and retain an amorphous structure, resulting in an efficient load bearing capacity of the inherently high strength amorphous alloy/metallic glass reinforcements. Overall, the mechanical properties of the developed new composites are promising and should be designed so as to compensate for the disadvantages faced by conventional MMCs and at the same time utilize the superior properties of the glassy materials. A synergistic effect of superior properties of the matrix and reinforcement is expected to give rise to novel and advanced hybrid materials.

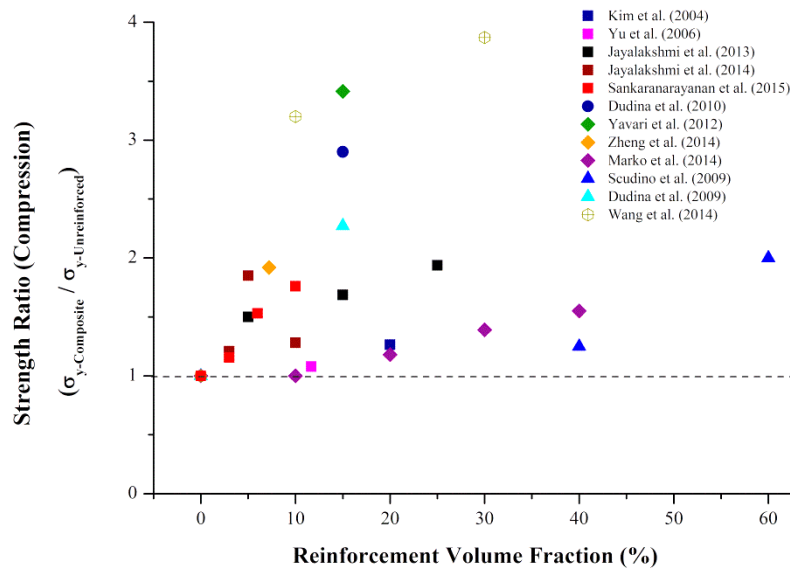


Figure 18. Compressive properties of amorphous alloy/metallic glass reinforced composites produced by different methods.

5. Conclusions

In most of the studies reviewed in this article, the incorporation of metallic glass reinforcement into light metal matrices (Al or Mg) enhanced the mechanical properties. The reported mechanical property enhancement was attributed to the inherent superior mechanical properties of the amorphous/metallic glass reinforcement. Further, the absence of interfacial reaction products (unlike conventional light metal matrix composites) also contributes towards the improvement of the composite properties. The method of processing the composite seems to play an influential role in defining the resulting properties. Composites produced by rapid processing methods such as high frequency induction sintering and rapid microwave sintering showed superior properties to those produced by conventional methods. Hence, by critically designing the nature and incorporation of metallic glass reinforcement with superior properties, the limitations faced by conventional metal matrix composite materials can be overcome.

Acknowledgments

The authors wish to acknowledge the funding support given by Ministry of Education, Singapore under grant “Singapore Ministry of Education Academic Research Fund—Tier 1” and WBS No: R-265-000-493-112, for carrying out this project.

Author Contributions

All authors contributed to the paper. Jayalakshmi Subramanian and Sankaranarayanan Seetharaman collected the data and prepared the manuscript. Manoj Gupta designed the scope of the paper. All authors discussed the conclusions and reviewed the manuscript.

Conflicts of Interest

The authors declare no conflict of interest.

References

1. Wang, W.-H.; Dong, C.; Shek, C. Bulk metallic glasses. *Mater. Sci. Eng. R Rep.* **2004**, *44*, 45–89.
2. Kainer, K.U. *Metal Matrix Composites: Custom-made Materials for Automotive and Aerospace Engineering*; John Wiley & Sons: Hoboken, NJ, USA, 2006.
3. Suresh, S.; Mortensen, A.; Needleman, A. *Fundamentals of Metal-matrix Composites*; Butterworth-Heinemann: Stoneham, MA, USA, 1993; p. 400.
4. Lee, M.; Kim, J.-H.; Park, J.; Kim, J.; Kim, W.; Kim, D. Fabrication of Ni-Nb-Ta metallic glass reinforced Al-based alloy matrix composites by infiltration casting process. *Scr. Mater.* **2004**, *50*, 1367–1371.
5. Yu, P.; Kim, K.; Das, J.; Baier, F.; Xu, W.; Eckert, J. Fabrication and mechanical properties of Ni-Nb metallic glass particle-reinforced Al-based metal matrix composite. *Scr. Mater.* **2006**, *54*, 1445–1450.
6. Eckert, J.; Calin, M.; Yu, P.; Zhang, L.; Scudino, S.; Duhamel, C. Al-based alloys containing amorphous and nanostructured phases. *Rev. Adv. Mater. Sci.* **2008**, *18*, 169–172.
7. Jayalakshmi, S.; Gupta, S.; Sankaranarayanan, S.; Sahu, S.; Gupta, M. Structural and mechanical properties of Ni₆₀Nb₄₀ amorphous alloy particle reinforced Al-based composites produced by microwave-assisted rapid sintering. *Mater. Sci. Eng. A* **2013**, *581*, 119–127.
8. Scudino, S.; Liu, G.; Prashanth, K.; Bartusch, B.; Surreddi, K.; Murty, B.; Eckert, J. Mechanical properties of Al-based metal matrix composites reinforced with Zr-based glassy particles produced by powder metallurgy. *Acta Mater.* **2009**, *57*, 2029–2039.
9. Dudina, D.; Georgarakis, K.; Aljerf, M.; Li, Y.; Braccini, M.; Yavari, A.; Inoue, A. Cu-based metallic glass particle additions to significantly improve overall compressive properties of an Al alloy. *Compos. Part A Appl. Sci. Manuf.* **2010**, *41*, 1551–1557.
10. Aljerf, M.; Georgarakis, K.; Louzguine-Luzgin, D.; Le Moulec, A.; Inoue, A.; Yavari, A. Strong and light metal matrix composites with metallic glass particulate reinforcement. *Mater. Sci. Eng. A* **2012**, *532*, 325–330.
11. Zheng, R.; Yang, H.; Liu, T.; Ameyama, K.; Ma, C. Microstructure and mechanical properties of aluminum alloy matrix composites reinforced with Fe-based metallic glass particles. *Mater. Des.* **2014**, *53*, 512–518.
12. Markó, D.; Prashanth, K.; Scudino, S.; Wang, Z.; Ellendt, N.; Uhlenwinkel, V.; Eckert, J. Al-based metal matrix composites reinforced with Fe_{49.9}Co_{35.1}Nb_{7.7}B_{4.5}Si_{2.8} glassy powder: Mechanical behavior under tensile loading. *J. Alloys Compd.* **2014**, *615*, S382–S385.
13. Wang, Z.; Tan, J.; Sun, B.; Scudino, S.; Prashanth, K.; Zhang, W.; Li, Y.; Eckert, J. Fabrication and mechanical properties of Al-based metal matrix composites reinforced with Mg₆₅Cu₂₀Zn₅Y₁₀ metallic glass particles. *Mater. Sci. Eng. A* **2014**, *600*, 53–58.

14. Fujii, H.; Sun, Y.; Inada, K.; Ji, Y.; Yokoyama, Y.; Kimura, H.; Inoue, A. Fabrication of Fe-based metallic glass particle reinforced al-based composite materials by friction stir processing. *Mater. Trans.* **2011**, *52*, 1634–1640.
15. Dudina, D.; Georgarakis, K.; Li, Y.; Aljerf, M.; LeMoulec, A.; Yavari, A.; Inoue, A. A magnesium alloy matrix composite reinforced with metallic glass. *Compos. Sci. Technol.* **2009**, *69*, 2734–2736.
16. Jayalakshmi, S.; Sahu, S.; Sankaranarayanan, S.; Gupta, S.; Gupta, M. Development of novel Mg-Ni₆₀Nb₄₀ amorphous particle reinforced composites with enhanced hardness and compressive response. *Mater. Des.* **2014**, *53*, 849–855.
17. Sankaranarayanan, S.; Shankar, H.; Jayalakshmi, S.; Nguyen, Q.; Gupta, M. Development of high performance magnesium composites using Ni₅₀Ti₅₀ metallic glass reinforcement and microwave sintering approach. *J. Alloys Compd.* **2015**, *627*, 8.

© 2015 by the authors; licensee MDPI, Basel, Switzerland. This article is an open access article distributed under the terms and conditions of the Creative Commons Attribution license (<http://creativecommons.org/licenses/by/4.0/>).